Rigid-Rod β-Barrel Ion Channels with Internal "Cascade Blue" Cofactors − Catalysis of Amide, Carbonate, and Ester Hydrolysis

Abhigyan Som[a] and Stefan Matile*[a]

Keywords: Bioorganic chemistry / Catalysis / Ion channels / Molecular recognition / Supramolecular chemistry

The pyrene-1,3,6-trisulfonate scaffold is introduced as an internal cofactor for histidine-rich *p*-octiphenyl β-barrels with catalytic and ion channel activity to mediate binding and conversion of otherwise inaccessible benzaldehyde substrates. Up to 170,000-fold accelerations of amide, ester, and carbonate hydrolysis, high substrate diversity, high chemoselectivity, and absence of enantioselectivity are reported.

Introduction

"Cascade Blues" (CBs) are classical fluorescent probes in chemistry and biology.[1−3] More recently, we suggested that the planar, rigid, and, of course, fluorescent CB-scaffold may also be of interest in supramolecular architecture.[4] In this study we exploit the CB·H^4 recognition motif[5] by the introduction of CB-hydrazides as internal cofactors[6] of H^4-rich *p*-octiphenyl β-barrel ion channels **1** (Figures 1 and 2) for binding and conversion of otherwise inaccessible substrates by reversible hydrazone formation.[7] The reported substantial accelerations of amide, ester, and carbonate hydrolysis by barrel **1** confirm the usefulness of the CB·H^4 motif in supramolecular catalysis[8] and beyond.

***p*-Oligophenyl β-Barrels:** Rigid-rod[9] β-barrels[10] such as **1** are man-made barrel-stave supramolecules.[11] *p*-Oligophenyls are privileged "staves"[12] because the axial, nonplanar arane-arene turns preorganize the desired cylindrical self-assembly and hinder the alternative supramolecular polymerization through linear self-assembly. The key role of the β-sheet "hoops" in *p*-oligophenyl β-barrels is to define the chemical and physical properties of the inner and outer barrel surfaces.[4,13−15] The sequence LHLHL in barrel **1** was chosen to provide external leucine arrays and H-quadruplets along the central hydrophilic channel for internal CB·H^4 recognition.[4,5]

The synthesis of monomeric *p*-octiphenyl **1*m*** has been reported.[4] According to atomic force microscopy (AFM),[16] cryoTEM,[16] and various spectroscopic structural and functional studies,[4,16−18] aqueous *p*-octiphenyls **1*m*** self-assemble into β-barrel **1** at nanomolar concentrations and transform into *p*-octiphenyl β-fibrils at micromolar levels (Figure 1).[19] Various lines of evidence − such as, for example, linear concentration dependence of transport[17] and milieu-independent esterase activity[4] − support an identical suprastructure for β-barrel **1** in water and in bilayer membranes. Intermediate internal charge repulsion (*ICR*) at $4 < pH < 6$ is required to stabilize the aqueous space within *p*-octiphenyl β-barrels.[17] The internal diameter calculated from single-channel conductance[4] is compatible with molecular models.[15b] The relatively poor stability of **1** has been shown by its short single-channel lifetime in membranes[4] and denaturation experiments in water.[18] Contraction of LHLHL-barrel **1** into homologous LHL-tetramer gives the expected reduction in internal diameter[20] and an increase in stability[20] without violation of the underlying *ICR* rule.[17]

The CB·H^4 Recognition Motif: Supramolecule **1** exhibits substantial ion channel,[4] esterase,[4] RNase,[18] and fibrillogenic activity.[16] Most relevantly for this study, rigid-rod β-barrel **1** is known to hydrolyze CB-acetate in water and in bilayer membranes with a proficiency $(k_{cat}/K_M)/k_{MeIm} = 9.6\cdot10^5$.[4] Turnover numbers (TONs) > 120 have been measured.[4,21] Poor esterolysis at high ionic strength, little dependence on substrate hydrophobicity, competitive inhibition by pyrene-1,3,6,8-tetrasulfonate (PTS), and bell-shaped pH profile maximal at pH 5.5 *all* indicate that esterolytic activity originates from electrostatic binding of planar CB-substrates to matching H-quadruplets within *p*-octiphenyl barrels **1** (Figure 2).[4] Submicromolar K_M, K_i (PTS), and K_D values corroborate the significance of the CB·H^4 recognition motif.[4] The voltage dependence of CB-binding within ion channel **1** suggests that *association* to the first available *peripheral* H-quadruplet is the rate-limiting process.[4] The diameter of contracted LHL-tetramer (without H-quadruplets) is, as would be expected, insufficient for internal CB-binding.[20]

Taken together with results from multifunctional rigid-rod β-barrel ion channels with other internal active sites,[13−15] and in view of the lack of high-resolution struc-

[a] Department of Organic Chemistry, University of Geneva, 1211 Geneva 4, Switzerland
Fax: (internat.) +41−22/328-7396
E-mail: stefan.matile@chiorg.unige.ch

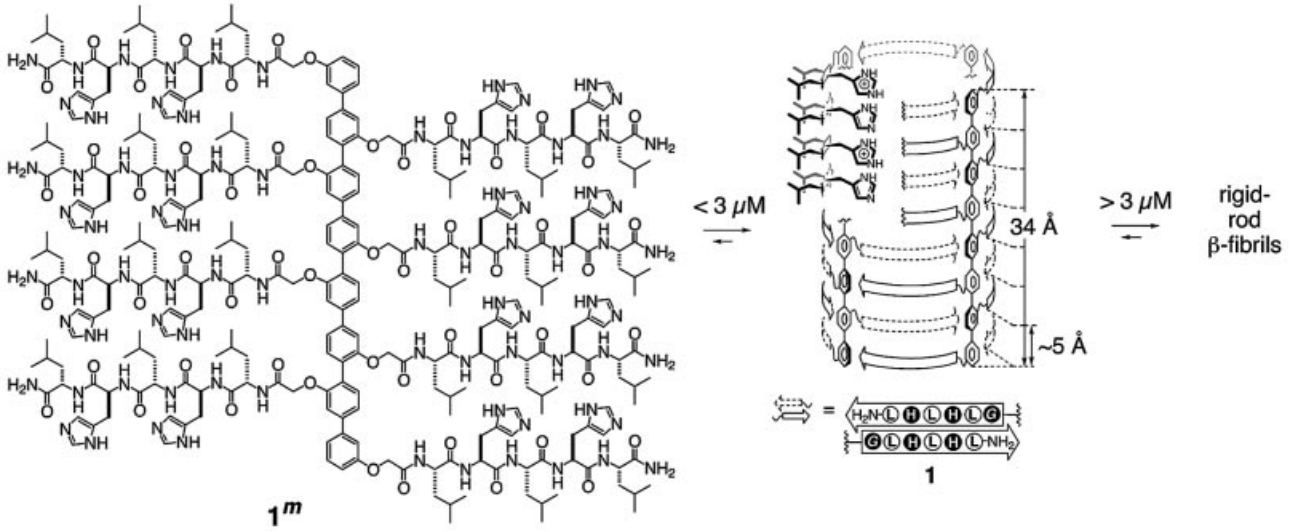

Figure 1. Self-assembly of *p*-octiphenyl **1*m*** into *p*-octiphenyl β-barrel ion channels **1** ($c < 3$ μM) and *p*-octiphenyl β-fibrils ($c > 3$ μM) in water; tetramer **1** is shown as a putative schematic cutaway suprastructure with vertical distances estimated from molecular models;[15b] β-strands are depicted as arrows pointing to the C-terminus, external α-hydroxy and α-amino acid residues (one-letter abbreviation, *G*: -OCH_2CO-) black on white and internal ones white on black; compare reference[16] for putative fibril suprastructures

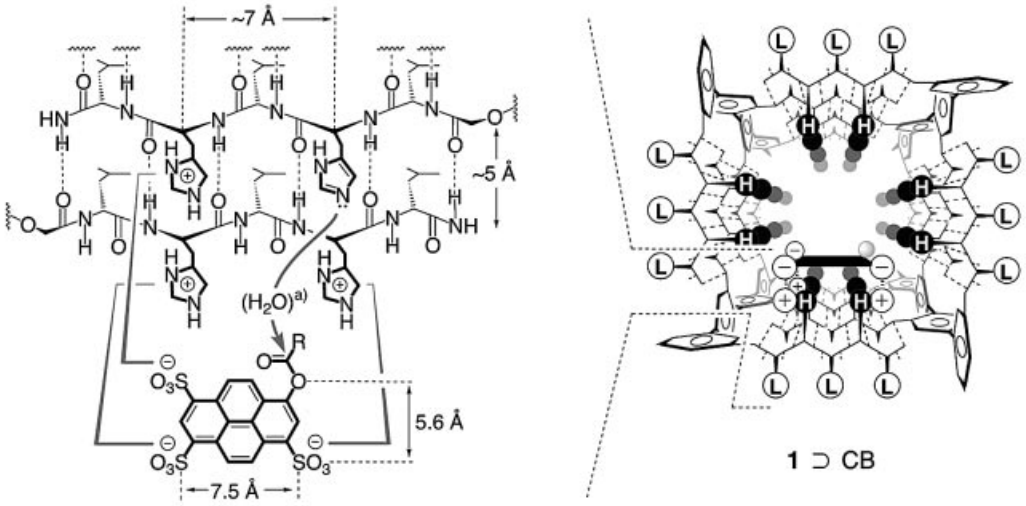

Figure 2. The CB·H^4 recognition motif;[1,5] previous results on hydrolysis of CB-esters [R = CH_3, $(CH_2)_2CH_3$, $(CH_2)_6CH_3$, $(CH_2)_{10}CH_3$] by barrel **1** implied formation of catalyst/substrate complexes **1** ⊃ CB with nanomolar K_M, K_I, as well as K_D by rate-limiting association of CB-substrates to the first available H^4-quadruplet at the channel entrance;[4] inclusion complex **1** ⊃ CB is depicted as an axial view with β-strands as solid (backbone) and dotted lines (hydrogen bonds); compare Figure 1 for structural details on barrel **1**; (a) no distinction is made between nucleophilic and base catalysis[21]

tural information from single crystals, both β-barrel suprastructure **1** (Figure 1) and internal CB·H^4 recognition (Figure 2) can be best appreciated as, at worst, productive working hypotheses that explain all characteristics of the multifunctionality of *p*-octiphenyl **1*m*** known today.

Design of "Cascade Blue" Cofactors: The objective of this study was to delineate the scope and limitations of the CB·H^4 recognition motif in supramolecular architecture and catalysis, with emphasis on amide hydrolysis (exemplified by substrate **2**, Scheme 1) as well as CB-cofactors.[6] CB-cofactors were conceived in order to obtain access to substrates that are otherwise not converted by barrel **1**. The expectation was that reversible binding to CB-cofactors would shuttle such substrates into the catalytic interior of supramolecule **1**, where they would be converted into product/cofactor complexes that would then dissociate to release the free products and reusable CB-cofactors.

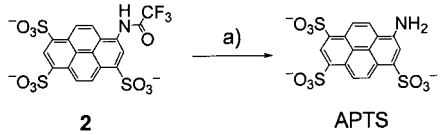

Scheme 1. Key: (a) + H_2O, -TFA

The design of CB-cofactors was developed with CB-hydrazide **3** as CB-cofactor, *p*-acetoxybenzaldehyde **4a** as substrate, and *p*-hydroxybenzaldehyde **5a** as product (Scheme 2). CB-hydrazide **3** was selected as cofactor because its treatment with substrate **4a** gives a substrate/cofactor conjugate **6a** that is quite stable in water under basic conditions but can be rapidly hydrolyzed under acidic conditions. Such controllable formation and hydrolysis of hydrazone **6a** compared favorably to the less stable aryl and alkyl imines accessible with alternative cofactors such as APTS and commercial CB-alkylamines, respectively.[1,7]

Operational CB·H^4 recognition should then direct substrate/cofactor conjugate **6a** into barrel **1**, where esterolysis by neighboring histidines and release of product/cofactor conjugate **7a** would follow (Scheme 2). *In principle*, all involved compounds **3**−**7** can be imagined to enter barrel **1**, and hydrazone formation and hydrolysis may occur either within the barrel or in the medium. For the initial assessment reported here, this rather complex system was simplified by eliminating the hydrazone formation step, to focus on esterolysis of substrate/cofactor conjugate **6a** to product/cofactor conjugate **7a** in competition with hydrazone hydrolysis to cofactor **3**.

Results and Discussion

Amide Hydrolysis

To explore the capacity of barrel **1** to catalyze CB(−like)·H^4-mediated amide hydrolysis, APTS-amide **2** was synthesized (Scheme 1). Substrate **2** and product APTS were detectable as clearly separated, broad peaks by ion-exchange high-pressure liquid chromatography (IE-HPLC)

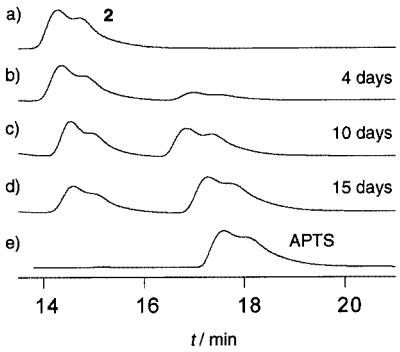

Figure 3. Conversion of amide **2** (a, 3 μM) into APTS (e) in the presence of barrel **1** (0.5 μM) in water (10 mM MES, pH 5.5) at ambient temperature detected after 4 (b), 10 (c), and 15 days (d) by IE-HPLC (without addition of perchlorate prior to injection, see Figure 7)

with a linear 0−1 M KCl gradient over 20 min (Figure 3, a and e). The origin of the second peak or shoulder with an unchanging absorption spectrum following substrate and product peak is unknown, but HSQC NMR spectroscopy allowed unacceptable sources such as impurities, regioisomers, and so on to be ruled out (see Exp. Sect.).

With this IE-HPLC assay, a $t_{1/2} \approx 11$ days was found for amide **2** in the presence of 0.5 μM barrel **1** at pH 5.5 and at ambient temperature (Figure 3, b−d and Table 1). In contrast, amide hydrolysis in the presence of 10 mM imidazole in place of 0.5 μM barrel gave a $t_{1/2} \approx 83$ days (Figure 4). Extrapolation to $t_{1/2} \approx 4548$ years with 0.5 μM imidazole suggested that barrel **1** accelerates amide hydrolysis by a quite remarkable factor of $1.5 \cdot 10^5$ (Table 1).[22]

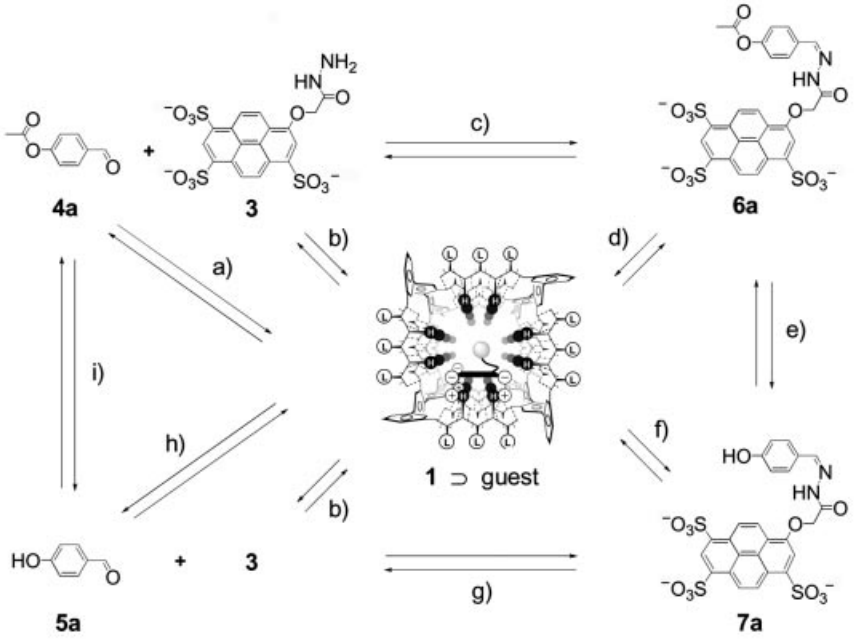

Scheme 2. Key: (a) Association of catalyst/substrate complex (+**1**). (b) Association of catalyst/cofactor complex (+**1**). (c) − H_2O. (d) Association of catalyst/cofactor/substrate complex (+**1**). (e) + H_2O, − AcOH. (f) Dissociation of catalyst/cofactor/product complex (−**1**). (g) + H_2O. (h) Dissociation of catalyst/product complex (−**1**). (i) + H_2O, − AcOH

Table 1. Catalysis of amide, ester, and carbonate hydrolysis by *p*-octiphenyl β-barrel **1**

Entry	Substrate [a]	R_t (min) [b]	Prod. [c]	Chemoselectivity **7**/**3** [d] barrel **1**	Chemoselectivity **7**/**3** [d] imidazole	$t_{1/2}$ (h) [e] barrel **1**	$t_{1/2}$ (uncat) [f] / $t_{1/2}$ (cat)	Relative activity [g]
1	**2**	14.5	APTS	-	-	270	$1.5\ 10^5$	88
2	**6a**	20.1	**7a**	100 / 0	100 / 0	0.7	$1.7\ 10^5$	100
3	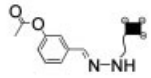 **6b**	20.5	**7b**	100 / 0	100 / 0	3.5	$9.3\ 10^4$	55
4	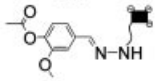 **6c**	19.9	**7c**	81 / 19	92 / 8	7.0	$5.7\ 10^4$	34
5	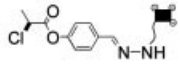 **6d**	23.5	**7a**	100 / 0	100 / 0	1.0 [h]	$3.4\ 10^4$	20
6	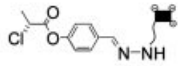 **6e**	23.5	**7a**	100 / 0	100 / 0	1.0 [h]	$3.4\ 10^4$	20
7	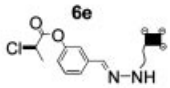 **6f**	24.0	**7b**	100 / 0	100 / 0	3.5 [h]	$3.3\ 10^4$	19
8	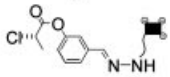 **6g**	24.0	**7b**	100 / 0	100 / 0	3.5 [h]	$3.3\ 10^4$	19
9	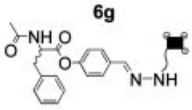 **6h**	26.1	**7a**	100 / 0	87 / 13	7.0	$2.5\ 10^4$	15
10	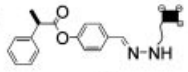 **6i**	33.5	**7a**	100 / 0	83 / 17	12.5	$8.0\ 10^3$	5
11	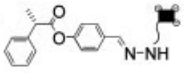 **6j**	33.5	**7a**	100 / 0	83 / 17	12.5	$8.0\ 10^3$	5
12	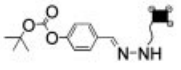 **6k**	25.0	**7a**	100 / 0	95 / 5	100 [h]	$5.0\ 10^3$	3
13	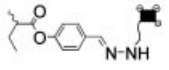 **6l**	25.5	**7a**	100 / 0	70 / 30	350	$2.3\ 10^3$	1
14	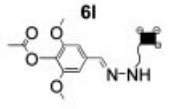 **6m**	19.0	**7m**	0 / 100	0 / 100	-	-	-
15	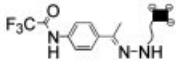 **6n**	19.7	**7n**	0 / 100	0 / 100	-	-	-

[a] Substrates (**2**, Scheme 1) and substrate/CB-cofactor conjugates (**6**, see Scheme 2 for CB and **6a**). [b] Substrate retention times R_t in IE-HPLC. [c] Products (APTS, Scheme 1) and product/CB-cofactor conjugates (**7**, see Scheme 2). [d] Product ratio determined by integration of IE-HPLC peaks for hydrazide **3** and phenols **7** for catalysis with barrel **1** (left column) and imidazole (right column). [e] Halflife time $t_{1/2}$ of 3 μM substrate in presence of 0.5 μM barrel **1**, pH 5.5, room temp. [f] Absolute activity of barrel **1** obtained by comparison of $t_{1/2}$ (cat) with 0.5 μM barrel **1** and $t_{1/2}$ (uncat) with 0.5 μM imidazole.[22] [g] $t_{1/2}$ (uncat)/$t_{1/2}$ (cat)-values relative to **6a** (entry 2, 100%). [h] Reaction temperature = 4 °C.

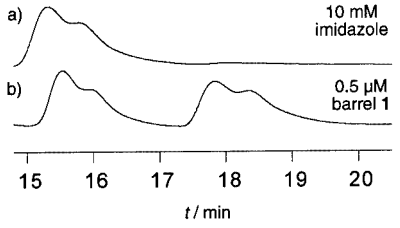

Figure 4. Conversion of amide **2** (3 μM, R_t = 15.5/15.9 min) into APTS (R_t = 17.8/18.3 min) in the presence of imidazole (a, 10 mM) and barrel **1** (a, 0.5 μM) in water (10 mM MES, pH 5.5) at ambient temperature, detected after 10 days by IE-HPLC (without addition of perchlorate prior to injection, see Figure 7)

"Cascade Blue" Cofactors

With experimental evidence of substantial acceleration of amide (Figure 4) and ester[4] hydrolysis by barrel **1** to hand, we set out to generalize the applicability of the underlying CB·H[4] recognition motif with the development of CB-cofactors as outlined in the Introduction (Scheme 2). As CB-cofactors are sensitive chromophores,[1−3] it was possible to detect CB-hydrazide **3** (Figure 5, a), substrate/cofactor conjugate **6a** (Figure 5, b), and product/cofactor conjugate **7a** (Figure 5, e) by ion-exchange HPLC as single peaks at the low concentrations relevant for activity of barrel **1** (Figure 1). In the presence of barrel **1** (0.5 μM), ester **6a** (3.0 μM) was transformed into phenol **7a** at pH 5.5 and ambient temperature with $t_{1/2} \approx 40$ min (Figure 5c, d). No hydrazide **3** was generated within this period of time. This barrel-catalyzed, cofactor-mediated esterolysis of **6a** was $1.7 \cdot 10^5$ times faster than the imidazole catalysis as described for APTS (Table 1).[21,22]

To assess the contribution of CB-cofactor **3** to this substantial acceleration, esterolysis of substrate **4a** by barrel **1** in the absence of cofactor was investigated. A modified assay was used for this purpose, because *p*-acetoxybenzaldehyde **4a** is a less sensitive chromophore than CB and because tetramer **1** transforms into fibrils above ≈ 1 μM barrel

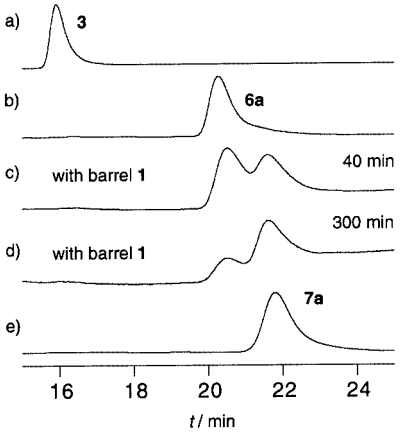

Figure 5. Conversion of substrate/cofactor conjugate **6a** (3 μM, b) into product/cofactor conjugate **7a** (e) rather than cofactor **3** (a) in the presence of barrel **1** (0.5 μM) in water (10 mM MES, pH 5.5) at ambient temperature, detected after 40 (c) and 300 min (d) by IE-HPLC (without addition of perchlorate prior to injection, see Figure 7)

concentration (Figure 1). The imidazole-catalyzed conversion of CB-free substrate **4a** into phenol **5a** was, however, readily detectable by absorption spectroscopy (Figure 6, a and c). The $t_{1/2}$ for esterolysis of *p*-acetoxybenzaldehyde **4a** with imidazole was in the range of that determined for substrate/cofactor conjugate **6a**. Barrel **1**, however, did not cause substantial hydrolysis of *p*-acetoxybenzaldehyde **4a** over a period of 19 hours (Figure 6, b).

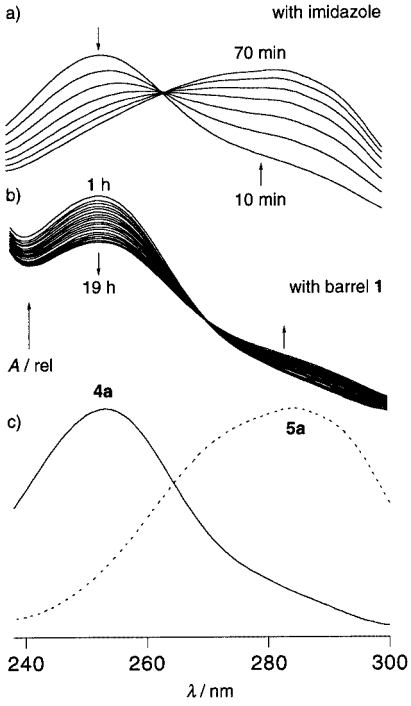

Figure 6. Conversion of substrate **4a** (100 μM, c, solid) into product **5a** (c, dotted) in the presence of imidazole (a, 80 mM) and barrel **1** (b, 0.5 μM) in water (10 mM MES, 100 mM KCl, pH 5.5) at ambient temperature, detected every 10 (a) and 60 min (b), respectively, by absorption spectroscopy

Substrate Diversity

Substrate/cofactor conjugates **6b−n** were synthesized and studied in order to elaborate on the substrate diversity accessible with CB-cofactors (Table 1). Hydrolysis of *m*-regioisomer **6b** in the presence of barrel **1** was about five times slower than with the original substrate/cofactor conjugate **6a** (Table 1, entries 3 versus 2). The catalytic activity of barrel **1** relative to imidazole was, however, quite similar for *m*- and *p*-regioisomers **6a** and **6b**. This trend was continued, with a tenfold deactivation and a reduction to 34% activity relative to **6a** by the *o*-methoxy π-donor in acetylvanillin **6c** (entries 4 versus 2). Further deactivation by another *o*-methoxy π-donor in acetate **6m** made esterolysis in the presence of 0.5 μM barrel **1** and 10 mM imidazole slower than the release of CB-cofactor **3** (entry 14).

Substitution of the original *p*- and *m*-acetates **6a** and **6b** with the 2-chloropropionates in **6d/e** and **6f/g**, respectively, accelerated esterolysis beyond HPLC-detectability at ambient temperature (entries 5−8). At 4 °C, both the difference in velocity and the similarity in relative activity of barrel **1**

for activated *p*- and *m*-isomers **6d/e** and **6f/g** were about as for the corresponding acetates **6a** and **6b**.

Endo and *Exo* Catalysis − A Speculative Working Hypothesis

The drop to 15% relative activity of barrel **1** with CB-phenylalanine **6h** may originate either from substrate hydrophobicity or from size (entry 9). Further decreases in relative activity with HTA-CBs **6i/j** (entries 10/11, Figure 7) and 2-methyl butyrate **6l** (entry 13) indicated that it is substrate hydrophobicity rather than size that influences substrate conversion.

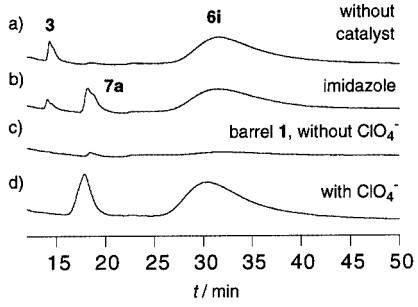

Figure 7. Conversion of substrate/cofactor conjugate **6i** (3 μM) into product/cofactor conjugate **7a** and cofactor **3** in water (a, 10 mM MES, pH 5.5) and in the presence of imidazole (b, 10 mM) or barrel **1** (c and d, 0.5 μM) at ambient temperature, detected after 6 (b) and 13 h (a, c, d) by IE-HPLC, with (d) and without (a−c) addition of perchlorate prior to sample injection

Practical difficulties hinted at the origin of the comparably poor catalytic activity of barrel **1** with hydrophobic CB-substrates (Figure 7, b−d). Whereas esterolysis of HTA-CB **6i** with imidazole could be followed as with more hydrophilic substrates **6a−g**, detectability with barrel **1** became unsatisfactory at identical substrate concentrations (Figure 7, b versus c). This suggested that barrel **1** was causing precipitation of more hydrophobic substrates. The most reasonable explanation of nonspecific, multiple substrate binding between hydrophobic outer surfaces of aggregated barrels turned out to be at least partially incorrect, because poorly soluble substrate/catalyst and product/catalyst complexes (Figure 7, c) could readily be redissolved with the aid of 2.4 M $NaClO_4$ (Figure 7, d). This perchlorate effect, well known from artificial RNases including barrel **1**,[18] also demonstrated operational CB·H^4 recognition with hydrophobic and more bulky substrates. We thus concluded that hydrophobic substrate/cofactor conjugates form *exo* CB·H^4 substrate/cofactor-barrel complexes in which only the CB-cofactor − but not the substrate itself − enters into the barrel (Figure 8). The poor activity of barrel **1** with *exo* catalysis, compared to efficient *endo* catalysis with hydrophilic substrates, would then be explicable in terms of reduced proximity of substrates and catalytic histidines. From a suprastructural point of view, we noted that poor (*exo*) conversion of more hydrophobic and good (*endo*) conversion of more hydrophilic substrates is in excellent agreement with the large and hydrophilic interior designed for barrel **1** (compare introduction).

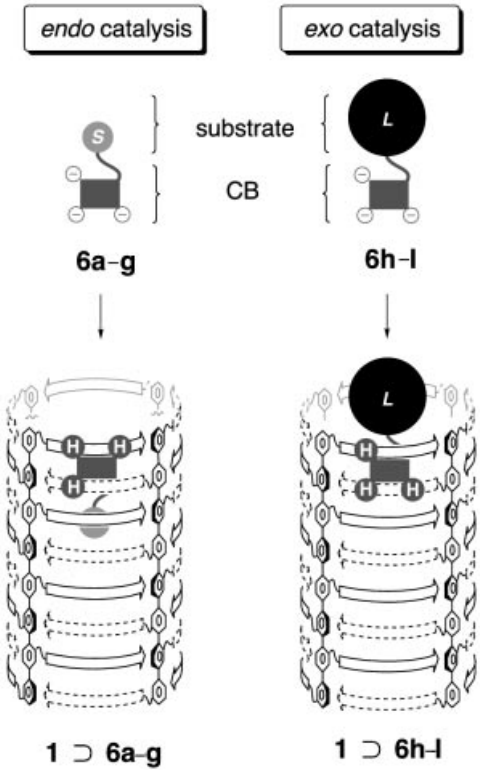

Figure 8. The *endo* catalysis with hydrophilic (gray) and small (*S*) substrate/cofactor conjugates **6a−g** and *exo* catalysis with hydrophobic (black) and large (*L*) hydrazones **6h−l** are envisionable as working hypotheses for better understanding of the results with barrel **1** (compare Table 1, Figures 1 and 2, and text)

Frequent coincidence of high R_t in IE-HPLC, poor (*exo*) catalysis, and substrate hydrophobicity was observed (Table 1). Transition from *endo* to *exo* catalysis may occur around $R_t \approx 24$ min and relative activity ≈ 15%. Exceptions from this simplistic "rule of thumb" as well as mixed *endo*/*exo* mechanisms cannot, of course, be ruled out. The *exo and endo catalysis must thus be considered strictly as a speculative working hypothesis that outlines two mechanistic possibilities, with the only intention being to stimulate future progress in the field.*

Enantioselectivity

No enantioselectivity was observed for putative *exo* catalysis with enantiomers **6i/j**, or for *endo* catalysis with *p*- and *m*-regioisomers **6d/e** and **6f/g** (Table 1). This lack of enantioselectivity with putative *endo* and *exo* catalysis was consistent with the expected high symmetry of both barrel interior and exterior. The synthesis of new *p*-octaphenyl β-barrels with increased asymmetry is continuing.

Chemoselectivity

The CB-cofactor design assumes that the rate of esterolysis exceeds that of hydrazone hydrolysis (Scheme 2). Cofactor release became detectable with, for example, hydrazone **6i** at pH 5.5 both in the presence and in the absence

of imidazole within about six hours (Figure 7, a and b). The presence of barrel **1** prevented hydrazide formation with hydrophobic substrates **6h**−**l** (Figure 7, d and Table 1). Although contributions from differences in the pK_a values of imidazole (7.0) and barrel **1** (< 6.0)[17] cannot be excluded, this chemospecificity most probably originated from the "heterogeneous" conditions observed for *exo* catalysis (Figure 7, c). Indeed, no increase in chemoselectivity was observed during *endo* catalysis with the more hydrophilic but deactivated substrates **6c** and **6m** (Table 1). Not surprisingly, hydrazone hydrolysis was faster than amide hydrolysis (Table 1, entries 1 and 15). Carbonate hydrolysis, however, occurred chemospecifically with comparably poor relative activity of barrel **1** (Table 1, entry 12). Both effects indicate "heterogeneous" *exo* catalysis with carbonate **6k**, although other contributions (e.g., differences in pK_a values, different contributions from acid catalysis) are possible as well.

Conclusion

The objective of this study was to delineate the usefulness of the CB·H^4 recognition motif in supramolecular architecture and catalysis. We report that CB-hydrazides can be used as cofactors that mediate binding and conversion of otherwise inaccessible benzaldehyde substrates within H^4-rich *p*-octaphenyl β-barrel ion channels. Consistent with their hydrophilic (and confined) interiors, esterolysis of cofactor-bound substrates is best with hydrophilic (and small) substrates (acceleration factors of between 33,000 and 170,000). Consistently with their symmetric interiors, esterolysis occurs without enantioselectivity. The less efficient hydrolysis of more hydrophobic CB-carbonates and CB-esters is chemospecific with regard to hydrazone hydrolysis (accelerations between 2,300 and 25,000). Among the best catalytic activities were obtained for amide hydrolysis (150,000-fold acceleration).[22]

This report expands the supramolecular functional plasticity of *p*-octiphenyl β-barrels with H^4-rich interiors to cover molecular recognition, ion-channel activity,[4] fibrillogenic activity,[16] and catalysis of RNA,[18] chemospecific but not enantioselective esterolysis, amide hydrolysis, and carbonate hydrolysis. The observed substrate diversity would be expected to be crucial for ongoing efforts to couple catalytic and ion-channel activity of *p*-octiphenyl β-barrels for the study of reactive intermediates on the single-molecule level.

Experimental Section

General Remarks: As mentioned in ref.[23], Supporting Information, APTS and **3** were purchased from Molecular Probes, salts and buffers from Sigma, commercial aldehyde/ketone substrates/products, (*S*)-2-chloropropanoic acid, (*R*)-2-chloropropanoic acid, (*S*)-2-phenylpropanoic acid, (*R*)-2-phenylpropanoic acid, 2-methylbutanoic acid, TFA, and imidazole from Fluka-Aldrich, and *N*-acetyl-L-phenylalanine (Ac-Phe-OH) from NovaBiochem. All compounds were of the best grade available and used as received.

HPLC measurements were performed with an Agilent series 1100 workstation (BinPump G1213A) with a NUCLEOGEN DEAE 60-7 ion-exchange column (120 × 8 mm, Macherey−Nagel & Co, Germany), and a diode array detector (Agilent series 1100, DAD G1215A); reported chromatograms were detected at 280 nm. UV/Vis spectra were recorded on a Varian Cary 1 Bio spectrophotometer equipped with stirred and thermostatted multicellholder.

Abbreviations: APTS = 8-aminopyrene-1,3,6-trisulfonate; CB = Cascade Blue = pyrene-8-X-oxy-1,3,6-trisulfonate; *G* = Gla: -OCH_2CO-, H-*G*-OH = glycolic acid; H^4 = histidine quadruplet (see ref.[5]); HBTU = *O*-benzotriazolyl-*N*,*N*,*N*′,*N*′-tetramethyluronium hexafluorophosphate; HPLC = high-pressure liquid chromatography; HTA = hydratropic acid; IE: ion-exchange; MeIm: 4(5)-methylimidazole; MES: 2-morpholinoethanesulfonic acid monohydrate.

1^3,2^3,3^2,4^3,5^2,6^3,7^2,8^3-Octa(Gla-Leu-His-Leu-His-Leu-NH_2)-*p*-octiphenyl (1*m*): Rod **1*m*** was synthesized, characterized, and purified as in ref.[4] of the Supporting Information. Stock solutions of **1*m*** were prepared in MeOH, and the *p*-octiphenyl concentration was confirmed by UV/Vis spectroscopy in MeOH [ε(*p*-octiphenyl) = 46.1 $mM^{-1}cm^{-1}$ (320 nm)].[24]

8-Trifluoroacetamidopyrene-1,3,6-trisulfonic Acid, Trisodium Salt (2): Trifluoroacetic anhydride (150 μL, 1.0 mmol) and triethylamine (TEA, 200 μL, 1.4 mmol) were added under nitrogen at 0 °C to a solution of 8-aminopyrene-1,3,6,-trisulfonic acid trisodium salt (APTS, 10 mg, 19.2 μmol) in DMF (1.00 mL). After stirring for 3 h in the dark at room temperature, the reaction mixture was concentrated in vacuo to give **2** [≈ quantitative (≈ 11.8 mg, confirmed from absorption at 380 nm and IE-HPLC (Figure 3) containing ca. 38 mg TEA (80%) and DMF (20%)] as a yellow, gummy liquid, which was used without purification. ^{1}H NMR (500 MHz, CD_3OD, 25 °C): δ [ppm] = 8.34 (d, $^3J_{H,H}$ = 8.3 Hz, 1 H, C(9)−H, HSQC to 124.2), 8.77 [s, 1 H, C(7)−H, HSQC to 125.6), 9.38−9.30 [m, 3 H, C(4)−H, C(5)−H, C(10)−H, HSQC to 128.6, 128.2, 127.6), 9.39 [s, 1 H, C(2)−H, HSQC to 126.3]. ^{13}C NMR (125 MHz, CD_3OD, 25 °C): δ [ppm] = 118.0 (q, $^1J_{C,F}$ = 288 Hz), 123.4 (s), 124.2 (d), 125.6 (d), 125.6 (s), 126.3 (d), 126.6 (s), 126.7 (s), 127.6 (d), 128.2 (d), 128.5 (s), 128.6 (d), 129.8 (s), 130.1 (s), 140.3 (s), 140.5 (s), 141.7 (s), 162.4 (q, $^2J_{C,F}$ = 35 Hz). MS (ESI, CH_3OH): *m*/*z* = 552 [M^{3-} + 2 H^+]$^-$, 574 [M^{3-}+ H^+ + Na^+]$^-$, 596 [M^{3-} + 2 Na^+]$^-$.

4-Formylphenyl (*R*)-(+)-2′-Chloropropionate (4d). General Procedure A: HBTU (910 mg, 2.4 mmol), 4-hydroxybenzaldehyde (200 mg, 1.6 mmol), and triethylamine (500 μL, 3.2 mmol) were added at 0 °C to a solution of (*R*)-(+)-2-chloropropionic acid (175 μL, 2.0 mmol) in DMF (3 mL). After stirring for 30 minutes in the dark at room temperature, the reaction mixture was diluted with CH_2Cl_2 (20 mL), extracted with 1 M aqueous $KHSO_4$ (1 × 20 mL), brine (1 × 20 mL), saturated aqueous $NaHCO_3$ (2 × 20 mL), and brine (1 × 20 mL), dried with Na_2SO_4, and concentrated in vacuo. Purification of the crude product by column chromatography (pentane/ethyl acetate 4:1, R_f = 0.3) yielded pure **4d** (95 mg, 28%) as a yellow liquid. Partial hydrolysis during column chromatography accounted for the modest yield. $[\alpha]_D^{20}$ = +1.00 (*c* = 1.98 in CH_2Cl_2). IR ($CHCl_3$): $\tilde{\nu}$ [cm^{-1}] = 3030 m, 2831 m, 2742 w, 1915 w, 1768 s, 1703 s, 1601 m, 1503 m, 1449 m, 1383 m, 1339 m, 1298 m, 1235 s, 1204 s, 1158 s, 1074 s, 859 s, 748 s. ^{1}H NMR (400 MHz, $CDCl_3$, 25 °C): δ [ppm] = 1.85 [d, $^3J_{H,H}$ = 7.1 Hz, 3 H, C(3′)−H], 4.66 [q, $^3J_{H,H}$ = 7.1 Hz, 1 H, C(2′)−H], 7.33 [br. d, $^3J_{H,H}$ = 8.0 Hz, 2 H, C(2)−H, C(6)−H], 7.95 [br. d, $^3J_{H,H}$ = 8.0 Hz, 2 H, C(3)−H, C(5)−H], 10.01 (s, 1 H, C*H*O). ^{13}C NMR (100 MHz, $CDCl_3$, 25

°C): δ [ppm] = 21.5 (q), 52.5 (d), 122.6 (d × 2), 131.7 (d × 2), 134.8 (s), 155.3 (s), 168.4 (s), 191.3 (d). HRMS (EI): *m/z* for $C_{10}H_9ClO_3$: calcd. 212.0240; found 212.0262; $C_{10}H_9ClO_3$ (212.63): C 56.49, H 4.27; found C 56.76, H 4.39.

4-Formylphenyl (*S*)-(−)-2′-Chloropropionate (4e): (*S*)-(−)-2-Chloropropionic acid (175 μL, 2.0 mmol) was converted into pure **4e** (110 mg, 32%) by procedure A. Analytical data were identical with those for **4d**, except for $[\alpha]_D^{20} = -1.08$ ($c = 6.08$ in CH_2Cl_2).

3-Formylphenyl (*R*)-(+)-2′-Chloropropionate (4f): (*R*)-(+)-2-Chloropropionic acid (175 μL, 2.0 mmol) was converted by procedure A and purified by column chromatography (pentane/ethyl acetate 4:1, $R_f = 0.3$) to give **4f** (102 mg, 30%) as a slightly yellow liquid. Partial hydrolysis during column chromatography accounted for the modest yield. $[\alpha]_D^{20} = +15.4$ ($c = 8.50$ in CH_2Cl_2). IR ($CHCl_3$): ṽ [cm^{-1}] = 3032 m, 2840 w, 2737 w, 1769 s, 1703 s, 1590 m, 1483 w, 1448 m, 1383 m, 1341 w, 1236 s, 1153 s, 1074 m, 1001 w, 923 m, 898 w, 801 m, 678 s, 644 w. ^{1}H NMR (400 MHz, $CDCl_3$, 25 °C): δ [ppm] = 1.84 [d, $^3J_{H,H}$ = 7.1 Hz, 3 H, C(3′)−H], 4.66 [q, $^3J_{H,H}$ = 7.1 Hz, 1 H, C(2′)−H], 7.41 [ddd, $^3J_{H,H}$ = 7.7, $^4J_{H,H}$ = 2.5, $^4J_{H,H}$ = 2.5 Hz, 1 H, C(6)−H], 7.58 [dd, $^3J_{H,H}$ = 7.7, $^3J_{H,H}$ = 7.7 Hz, 1 H, C(5)−H], 7.66 [dd, $^4J_{H,H}$ = 2.5, $^4J_{H,H}$ = 2.5 Hz, 1 H, C(2)−H], 7.79 [ddd, $^3J_{H,H}$ = 7.7, $^4J_{H,H}$ = 2.5, $^4J_{H,H}$ = 2.5 Hz, 1 H, C(4)−H], 10.22 (s, 1 H, C*H*O). ^{13}C NMR (100 MHz, $CDCl_3$, 25 °C): δ [ppm] = 21.6 (q), 52.5 (d), 122.1 (d), 127.7 (d), 128.3 (d), 130.7 (d), 138.2 (s), 151.3 (s), 168.8 (s), 191.4 (d). HRMS (EI): *m/z* for $C_{10}H_9ClO_3$: calcd. 212.0240; found 212.0258; $C_{10}H_9ClO_3$ (212.63): C 56.49, H 4.27; found C 56.39, H 4.32.

3-Formylphenyl (*S*)-(−)-2′-Chloropropionate (4g): (*S*)-(−)-2-Chloropropionic acid (175 μL, 2.0 mmol) was converted into pure **4g** (98 mg, 29%) by procedure A. Analytical data were identical with those for **4f**, except for $[\alpha]_D^{20} = -15.3$ ($c = 7.99$ in CH_2Cl_2).

(±)-*N*-α-Acetylphenylalanine 4-Formylphenyl Ester (4h). General Procedure B: 1-(3-Dimethylaminopropyl)-3-ethylcarbodiimide−HCl (EDC·HCl, 1.00 g, 5.21 mmol), 4-hydroxybenzaldehyde (200 mg, 1.64 mmol), and triethylamine (0.80 mL, 5.70 mmol) were added at 0 °C to a solution of Ac-D-Phe-OH (500 mg, 2.41 mmol) in CH_2Cl_2 (10 mL). After stirring in the dark at room temperature for 6 h, the reaction mixture was diluted with CH_2Cl_2 (20 mL), extracted with saturated aqueous $NaHCO_3$ (1 × 20 mL), brine (1 × 20 mL), 1 M aqueous $KHSO_4$ (1 × 20 mL), and brine (1 × 20 mL), dried with Na_2SO_4, and concentrated in vacuo. Purification of the crude product by column chromatography (pentane/ethyl acetate 1:2, $R_f = 0.3$) yielded **4h** (395 mg, 53%) as a colorless solid. Partial hydrolysis during column chromatography accounted for the modest yield. $[\alpha]_D^{20} = +0.05$ ($c = 9.6$ in CH_2Cl_2); m.p. 119.5−120.2 °C. IR ($CHCl_3$): ṽ [cm^{-1}] = 3620 w, 3301 m, 3011 s, 1765 s, 1700 s, 1678 s, 1601 m, 1514 m, 1426 m, 1218 s, 1158 m, 1053 m, 927 m, 768 s, 664 m. ^{1}H NMR (400 MHz, $CDCl_3$, 25 °C): δ [ppm] = 2.05 (s, CH_3), 3.22−3.32 [m, 2 H, C(β)−H], 5.10 [dd, $^3J_{H,H}$ = 13.6, $^3J_{H,H}$ = 6.6 Hz, 1 H, C(α)−H], 6.11 (br. s, 1 H, N−H, exchange with D_2O), 7.16 [br. d, $^3J_{H,H}$ = 8.4 Hz, 2 H, C(2)−H, C(6)−H], 7.24 [br. dd, $^3J_{H,H}$ = 8.1, $^4J_{H,H}$ = 1.8 Hz, 2 H, C(2′)−H, C(6′)−H], 7.38−7.28 [m, 3 H, C(3′)−H, C(4′)−H, C(5′)−H], 7.90 [br. d, $^3J_{H,H}$ = 8.4 Hz, 2 H, C(3)−H, C(5)−H], 9.98 (s, 1 H, C*H*O). ^{13}C NMR (100 MHz, $CDCl_3$, 25 °C): δ [ppm] = 23.0 (q), 37.8 (t), 53.5 (d), 122.1 (d × 2), 127.5 (d), 128.8 (d × 2), 129.3 (d × 2), 131.2 (d × 2), 132.3 (s), 134.2 (s), 135.2 (s), 154.7 (s), 169.8 (s), 190.7 (d). MS (ESI, $CHCl_3$): *m/z* = 334 [M + Na]$^+$; $C_{18}H_{17}NO_4$ (311.34): C 69.44, H 5.50, N 4.50; found C 69.27, H 5.56, N 4.33. Ac-L-Phe-OH (500 mg, 2.41 mmol) was converted into pure **4h** (376 mg, 50%) by procedure B; analytical data were identical with those for the Ac-D-Phe-OH used as starting material, including $[\alpha]_D^{20} = +0.06$ ($c = 9.6$ in CH_2Cl_2).

4-Formylphenyl (*R*)-(−)-2′-Phenylpropionate (4i): (*R*)-(−)-2-Phenylpropionic acid (48 mg, 0.32 mmol) was converted by procedure A and purified by column chromatography (pentane/ethyl acetate 4:1, $R_f = 0.3$) to give **4i** (60 mg, 90%) as a colorless liquid, which solidified between 0 °C and room temperature. $[\alpha]_D^{20} = -77.5$ ($c = 8.04$ in CH_2Cl_2). IR ($CHCl_3$): ṽ [cm^{-1}] = 3022 m, 1758 s, 1702 s, 1601 m, 1504 w, 1454 w, 1225 m, 1208 s, 1157 m, 1138 w, 1074 w, 788 s, 764 s, 744 s, 729 m, 699 m, 666 w. ^{1}H NMR (400 MHz, $CDCl_3$, 25 °C): δ [ppm] = 1.66 (d, $^3J_{H,H}$ = 7.1 Hz, 3 H, C(3′)−H], 4.02 (q, $^3J_{H,H}$ = 7.1 Hz, 1 H, C(2′)−H], 7.20 [br. d, $^3J_{H,H}$ = 8.6 Hz, 2 H, C(2)−H, C(6)−H], 7.42−7.31 [m, 5 H, C(Ar)−H], 7.89 [br. d, $^3J_{H,H}$ = 8.6 Hz, 2 H, C(3)−H, C(5)−H], 10.21 (s, 1 H, C*H*O). ^{13}C NMR (100 MHz, $CDCl_3$, 25 °C): δ [ppm] = 18.8 (q), 46.1 (d), 122.9 (d × 2), 128.2 (d × 3), 129.1 (d × 2), 131.5 (d × 2), 134.3 (s), 140.1 (s), 155.9 (s), 172.8 (s), 191.3 (d). HRMS (EI): *m/z* for $C_{16}H_{14}O_3$: calcd. 254.0943; found 254.0958; $C_{16}H_{14}O_3$ (254.28): C 75.58, H 5.55; found C 75.57, H 5.57.

4-Formylphenyl (*S*)-(+)-2′-Phenylpropionate (4j): (*S*)-(+)-2-Phenylpropionic acid (48 mg, 0.32 mmol) was converted into pure **4j** (52 mg, 87%) by the procedure used for **4i**. Analytical data were identical with those for **4i**, except for $[\alpha]_D^{20} = +73.2$ ($c = 4.58$ in CH_2Cl_2).

4-Formylphenyl (±)-2′-Methylbutanoate (4k): (±)-2-Methylbutanoic acid (500 mg, 2.41 mmol) was converted by procedure B and purified by column chromatography (pentane/ethyl acetate 4:1, $R_f = 0.3$) to give **4k** (164 mg, 46%) as a colorless solid. Partial hydrolysis during column chromatography accounted for the modest yield. M.p. 79.5−80.0 °C. IR ($CHCl_3$): ṽ [cm^{-1}] = 3029 w, 2974 w, 2939 w, 1755 s, 1702 s, 1605 m, 1505 w, 1462 m, 1419 w, 1208 s, 1159 s, 1110 m, 905 w, 786 s, 764 s, 752 w, 746 m, 732 s, 700 m. ^{1}H NMR (400 MHz, $CDCl_3$, 25 °C, TMS): δ [ppm] = 1.05 [t, $^3J_{H,H}$ = 7.1 Hz, 3 H, C(4′)−H], 1.33 [d, $^3J_{H,H}$ = 6.9 Hz, 3 H, C(2′)−CH_3], 1.67 [ddq, $^2J_{H,H}$ = 13.6, $^3J_{H,H}$ = 7.1, $^3J_{H,H}$ = 6.8 Hz, 1 H, C(3′)−H], 1.87 [ddq, $^2J_{H,H}$ = 13.6, $^3J_{H,H}$ = 7.1, $^3J_{H,H}$ = 6.8 Hz, 1 H, C(3′)−H], 2.68 [tq, $^3J_{H,H}$ = 6.9, $^3J_{H,H}$ = 6.8 Hz, 1 H, C(2′)−H], 7.23 [br. d, $^3J_{H,H}$ = 8.8 Hz, 2 H, C(2)−H, C(6)−H], 8.17 [br. d, $^3J_{H,H}$ = 8.8 Hz, 2 H, C(3)−H, C(5)−H], 10.02 (s, 1 H, C*H*O). ^{13}C NMR (100 MHz, $CDCl_3$, 25 °C): δ [ppm] = 11.6 (q), 16.5 (q), 26.7 (t), 41.2 (d), 121.8 (d × 2), 131.8 (d × 2), 133.9 (s), 155.6 (s), 174.5 (s), 191.0 (d). MS (CI): *m/z* = 206 [M]$^+$; $C_{12}H_{14}O_3$ (206.24): C 69.89, H 6.84; found C 69.03, H 6.34.

CB-Hydrazones: Aldehydes or ketones (**4a−4n, 5a−5n**, 100 mM in DMSO, 20 μL) and CB-hydrazide **3** (20 μL in DMSO, 50 mM) were mixed and placed on a shaker at ambient temperature in the dark for 4−6 h. The mixture was then diluted with DMSO (3.3 mL) to obtain a 300 μM hydrazone stock solution. Hydrazide consumption was monitored by addition of 20 μL of this solution to 2.0 mL buffer (10 mM MES, pH 5.5), and 400 μL of this solution were injected into the HPLC machine and separated on a NUCLEOGEN DEAE 60−7 ion-exchange column with a linear gradient from 80% 20 mM KH_2PO_4, pH 5.5, 20% acetonitrile to 80% 1 M KCl, 20 mM KH_2PO_4, pH 5.5, 20% acetonitrile in 20 min, a flow rate of 1 mL/min. Retention times for hydrazones **6a−6n** and **7a−7n** not specified in Table 1 and Figure 3 were as follows: **7b**: R_t = 21.9 min; **7c**: R_t = 21.1 min; **7m**: R_t = 19.6 min; **7n**: R_t = 20.1 min.

Amide, Ester, and Carbonate Hydrolysis, IE-HPLC Assay. With/Without 0.5 μM Barrel 1: Substrate (**2**, **6a−n** 300 μM in DMSO, 20 μL) and either rod **1*m*** (250 μM in MeOH,16 μL) or MeOH (negative control, 20 μL) were added to buffer (10 mM MES, pH 5.5, 2.0 mL). The reaction mixture was distributed among five vials (400 μL each), which were placed on a shaker at ambient temperature or at 4 °C (Table 1) in the dark. After each appropriate period of time, the content of one vial was injected into the HPLC machine and separated on a NUCLEOGEN DEAE 60-7 ion-exchange column with a linear gradient from 80% 20 mM KH_2PO_4, pH 5.5, 20% acetonitrile to 80% 1 M KCl, 20 mM KH_2PO_4, pH 5.5, 20% acetonitrile in 20 min, at a flow rate of 1 mL/min. Peaks for all compounds were assigned by comparison and coinjection with separately prepared samples containing pure APTS, **2**, **3**, **6a−6m**, **7a**, **7b**, **7m**, and **7n**. Addition of $NaClO_4$ (10.0 M in 10 mM MES, pH 5.5, 125 μL) directly before HPLC analysis was useful to improve detection.

With 10 μM imidazole: Amide **2** (300 μM in DMSO, 20 μL) or hydrazones **6a−n** (300 μM in DMSO, 20 μL) were added to buffer (10 mM imidazole, pH 5.5, 2.0 mL); samples were then treated as those with/without barrel **1**. Since $t_{1/2} = 1/c{\cdot}k$ for second order reactions, halflife times $t_{1/2}'$ measured for 10 mM imidazole were converted into $t_{1/2}$ (uncat) for 0.5 μM imidazole in Table 1 by use of $t_{1/2}$ (uncat) = $t_{1/2}' \times 20{,}000$.

Esterolysis; UV/Vis Spectroscopy Kinetics: The spectra of pure ester **4a** (100 μM) and phenol **5a** (100 μM) in 10 mM MES, 100 mM KCl, pH 5.5, were determined (Figure 6, c). Then, ester **4a** (2.5 mM in EtOH,40 μL) and (b) rod **1*m*** (100 μM in MeOH, 20 μL) or (a) imidazole (2 M in H_2O, pH 5.5, 40 μL) were added to 1.0 mL buffer (10 mM MES, 100 mM KCl, pH 5.5) in UV/Vis cuvettes equipped with a magnetic stirrer bar. These cuvettes were placed in a thermostatted cell multiholder (25 °C), and UV/Vis spectra were measured every 10 min for (a) and every 60 min for (b).

Acknowledgments

We thank B. Baumeister and D. Gerard for assistance in organic synthesis, N. Sakai for advice and critical reading of the manuscript, D. Jeannerat, A. Pinto, and J.-P. Saulnier for NMR measurements, the group of F. Gülaçar for MS measurements, H. Eder for elemental analyses, and the Swiss NSF (2000-064818.01 and National Research Program "Supramolecular Functional Materials" 4047-057496) for financial support.

[1] Cascade Blue (CB) = pyrene-8-X-oxy-1,3,6-trisulfonate: R. P. Haugland, *Handbook of Fluorescent Probes and Research Chemicals, Ed. 6*, Molecular Probes, Eugene, OR, **1996**.
[2] O. S. Wolfbeis, E. Koller, *Anal. Biochem.* **1983**, *129*, 365−370.
[3] J. E. Whitaker, R. P. Haugland, P. L. Moore, P. C. Hewitt, M. Reese, R. P. Haugland, *Anal. Biochem.* **1991**, *198*, 119−130.
[4] B. Baumeister, N. Sakai, S. Matile, *Org. Lett.* **2001**, *3*, 4229−4232.
[5] Use of the following convention is suggested for convenience and clarity: X^4 or X-quadruplet stands for four juxtaposed amino acid residues (one-letter abbreviation) on one side of a two-stranded β-sheet that form an approximately planar rectangle of ≈ 5 Å × ≈ 7 Å; example: H-quadruplet in Figure 2.
[6] A cofactor is defined as "inorganic ion or coenzyme (small molecule tightly associated with an enzyme that participates in the reaction that the enzyme catalyzes, often by forming a covalent bond to the substrate) that is required for an enzymes activity" (B. Alberts, D. Bray, J. Lewis, M. Raff, K. Roberts, J. D. Watson, *Molecular Biology of the Cell*, 3rd Edn., Garland, New York, **1994**, G-6). Although consistent with the role of CB in this study, "cofactor" is used mainly for convenience and could be replaced by another term if desired.
[7] For recent use of hydrazones as alternatives to imines in "dynamic combinatorial libraries", see: [7a] R. L. E. Furlan, Y.-F. Ng, S. Otto, J. M. K. Sanders, *J. Am. Chem. Soc.* **2001**, *123*, 8876−8877. [7b] J. M. K. Sanders, *Pure Appl. Chem.* **2000**, *72*, 2265−2274. [7c] J.-M. Lehn, *Chem. Eur. J.* **1999**, *5*, 2455−2463.
[8] J. M. K. Sanders, *Chem. Eur. J.* **1998**, *4*, 1378−1383.
[9] Some rigid-rod molecules: [9a] K. Fuji, T. Furuta, K. Tanaka, *Org. Lett.* **2001**, *3*, 169−171. [9b] M. W. Read, J. Escobedo, D. M. Willis, P. A. Beck, R. M. Strongin, *Org. Lett.* **2000**, *2*, 3201−3204. [9c] K. Pieterse, J. A. J. M. Vekemans, H. Kooijman, A. L. Spek, E. W. Meijer, *Chem. Eur. J.* **2000**, *6*, 4597−4603. [9d] M. D. Levin, P. Kaszynski, J. Michl, *Chem. Rev.* **2000**, *100*, 169−234. [9e] P. F. H. Schwab, M. D. Levin, J. Michl, *Chem. Rev.* **1999**, *99*, 1863−1934.
[10] Some β-barrels: [10a] W. T. Taylor, *Nature* **2002**, *416*, 657−660. [10b] C. R. Calladine, A. Sharff, B. Luisi, *J. Mol. Biol.* **2001**, *305*, 603−618. [10c] D. Qi, C.-M. Tann, D. Haring, M. D. Distefano, *Chem. Rev.* **2001**, *101*, 3081−3112. [10d] N. Nagano, E. G. Hutchinson, J. M. Thornton, *Protein Sci.* **1999**, *8*, 2072−2084. [10e] S. K. Buchanan, *Curr. Opin. Struct. Biol.* **1999**, *9*, 445−461. [10f] D. R. Flower, *Biochem. J.* **1996**, *318*, 1−14. [10g] M. H. Hecht, *Proc. Natl. Acad. Sci. USA* **1994**, *91*, 8729−8730.
[11] S. Matile, *Chem. Soc. Rev.* **2001**, *30*, 158−167.
[12] Innovative scaffolds other than rigid rods in β-sheet architecture: [12a] H. Zeng, X. Yang, R. A. Flowers II, B. Gong, *J. Am. Chem. Soc.* **2002**, *124*, 2903−2910. [12b] Y. Hamuro, A. D. Hamilton, *Bioorg. Med. Chem.* **2001**, *9*, 2355−2363. [12c] R. Kaul, A. R. Angeles, M. Jäger, E. T. Powers, J. W. Kelly, *J. Am. Chem. Soc.* **2001**, *123*, 5206−5212. [12d] J. S. Nowick, *Acc. Chem. Res.* **1999**, *32*, 287−296, and references therein. [12e] T. Sazaki and M. Lieberman, *Protein Mimetics*, in: *Comprehensive Supramolecular Chemistry, Vol. 4*, (Ed.: Y. Murakami, Elsevier, Oxford, **1996**, 193−243.
[13] *p*-Octiphenyl β-barrels with internal aspartates: G. Das, S. Matile, *Proc. Natl. Acad. Sci. USA* **2002**, *99*, 5183−5188.
[14] *p*-Octiphenyl β-barrels with internal lysines: [14a] N. Sakai, S. Matile, *J. Am. Chem. Soc.* **2002**, *124*, 1184−1185. [14b] B. Baumeister, N. Sakai, S. Matile, *Angew. Chem.* **2000**, *112*, 2031−2034; *Angew. Chem. Int. Ed.* **2000**, *39*, 1955−1958. [14c] N. Sakai, B. Baumeister, S. Matile, *ChemBioChem.* **2000**, *1*, 123−125.
[15] *p*-Oligophenyl β-barrels with internal leucines: [15a] G. Das, S. Matile, *Chirality* **2001**, *13*, 170−176. [15b] B. Baumeister, S. Matile, *Chem. Eur. J.* **2000**, *6*, 1739−1749.
[16] G. Das, L. Ouali, M. Adrian, B. Baumeister, K. J. Wilkinson, S. Matile, *Angew. Chem.* **2001**, *113*, 4793−4797; *Angew. Chem. Int. Ed.* **2001**, *40*, 4657−4661.
[17] B. Baumeister, A. Som, G. Das, N. Sakai, F. Vilbois, D. Gerard, S. P. Shahi, S. Matile, *Helv. Chim. Acta* in press.
[18] B. Baumeister, S. Matile, *Macromolecules* **2002**, *35*, 1549−1555.
[19] Elaborating on the "intrinsic hydrophilic character of organic compounds", Hine and Mookerjee pointed out that the solubility of, for example, 2-methylpropane in water is 850 μM: [19a] J. Hine, P. K. Mookerjee, *J. Org. Chem.* **1975**, *40*, 292−298. Poly(HL) is insoluble in water: [19b] B. Barbier, A. Brack, *J. Am. Chem. Soc.* **1992**, *114*, 3511−3515.
[20] A. Som, N. Sakai, S. Matile, unpublished results.
[21] Please note that an acyl-imidazole intermediate is highly reactive at pH 5.5: W. P. Jencks, J. Carriuolo, *J. Biol. Chem.* **1959**, *234*, 1272−1285.
[22] The absolute activity of barrel **1** (i.e., the "*maximal activity*") is obtained by dividing $t_{1/2}$ (uncat) of 3 μM substrate in the presence of 0.5 μM imidazole (extrapolated from experimental values for 10 mM imidazole) by $t_{1/2}$ (cat) of 3 μM substrate with

0.5 μM barrel **1** under identical conditions. The absolute activity *of a single histidine residue* within barrel **1** (i.e., the "*minimal activity*") is 64 times lower than the values calculated for barrel **1** ($2.7 \cdot 10^3$ for **6a**, $2.3 \cdot 10^3$ for **2**, and so on, Table 1). The values calculated for barrel **1** (i.e., *maximal* rather than *minimal activities)* are more realistic, judged from previous detailed studies with CB-acetate reported in,[4] as well as preliminary results indicating that replacement of every second histidine in barrel **1** by an arginine residue does not significantly influence catalytic activity.

[23] N. Sakai, D. Gerard, S. Matile, *J. Am. Chem. Soc.* **2001**, *123*, 2517−2524.
[24] L. A. Weiss, N. Sakai, B. Ghebremariam, C. Ni, S. Matile, *J. Am. Chem. Soc.* **1997**, *119*, 12,142−12,149.

Received May 23, 2002
[O02275]